Low-Temperature Growth of Epitaxial β-SiC on Si(100) Using Supersonic Molecular Beams of Methylsilane[†]

Errol C. Sanchez[‡] and Steven J. Sibener*

The James Franck Institute and Department of Chemistry, The University of Chicago, 5640 S. Ellis Avenue, Chicago, Illinois 60637

Received: April 4, 2002; In Final Form: June 10, 2002

Epitaxial β-SiC films have been successfully grown on Si(100) at substrate temperatures considerably lower than those used during conventional CVD growth. This has been achieved using translationally energetic and spatially directed methylsilane delivered via seeded supersonic molecular beams. Methylsilane kinetic energy was found to dramatically affect both film morphology and growth behavior, as well as the enhancement of growth efficiency in the substrate temperature range 830−1030 K. Films obtained from thermal beams (0.079 eV) grow only through the facile mechanism involving the reaction of out-diffused silicon atoms with precursor species, identical to the growth of so-called "buffer layers" via the reactive conversion of the silicon surface. At moderately higher kinetic energies (0.45 eV), a second growth mechanism opens which operates in addition to the silicon out-diffusion process. Growth at the higher incident energy can grow thicker films, i.e., is not thickness-limited, and occurs with essentially the same rates with or without a buffer layer. The morphological evolution of films grown on bare substrates proceeds through a pitted buffer or transitional layer, which allows for the relaxation of strain due to lattice mismatch. The continuous, void-free films eventually obtained exhibit the doubly degenerate domain structure characteristic of cubic epitaxial material growing nearly two-dimensionally. Furthermore, remarkable square-pyramidally shaped and azimuthally aligned isolated three-dimensional features identified as Si islands are observed to grow simultaneously with the two-dimensional SiC film. Films grown below 900 K, though also epitaxial β-SiC, do not show these isolated three-dimensional features, and are much rougher than films grown above 900 K. These results emphasize that new, enhanced growth regimes for electronic materials deposition can be achieved by using high-intensity and velocity-tuned supersonic molecular beams to deliver kinetically accelerated neutral molecules for use as efficient growth precursors. These experiments also suggest that lower substrate thermal ranges may, for favorable cases, become accessible for growing high-quality films when using supersonic molecular beam epitaxy (SMBE) deposition methods.

I. Introduction

The strong influence that neutral reactant translational energy has in gas-phase and gas-surface processes is well-known. Atomic and molecular inelastic-scattering at surfaces, as well as molecular condensation and dissociative adsorption at hyperthermal energies, are examples where the outcome of such illustrative physical and chemical processes has been seen to be significantly altered by incident state translational energy.[1,2]

Within the last 15 years, potential technological applications utilizing kinetically activated chemistry in the field of semiconductor growth have been identified. This is a direct consequence of successful modulated-molecular beam studies which have emulated the gas-surface reaction environment used in technologically important semiconductor processes such as etching, chemical vapor deposition (CVD), and molecular beam epitaxy (MBE) within highly controlled ultrahigh vacuum environments.[3] In these experiments, reactant translational energy can be used as a control parameter when elucidating the kinetics and dynamics of the individual reaction steps which, taken together, comprise the overall mechanism for materials growth or removal. Efforts to actually exploit, in a systematic manner, neutral reactant translational energy as a semiconductor growth parameter accelerated from the mid 1990s through the use of supersonic molecular beam deposition techniques[4−17] as well as laser ablation/vaporization deposition techniques.[18−19]

In conventional materials growth processes, substrate temperature is typically the most important experimental control parameter during deposition. The low-temperature limit during epitaxy is dictated by the particular step in the growth process (chemisorption, surface diffusion, accommodation, incorporation, etc.) which has the highest thermodynamic constraint or kinetic barrier.[19] The potential of carrying out epitaxial growth by using translationally fast molecules to synthesize well defined, ordered, crystalline films at substrate temperatures lower than has been possible with conventional CVD and MBE techniques is intriguing, and potentially quite important, as problems associated with interdiffusion at critical interfaces may be diminished or mitigated. This possibility may be brought about by channeling translational energy to the relevant activated step such as dissociative adsorption, activated chemistry, or surface migration. Lower temperature processing is also advantageous as it may allow more thermally sensitive, but higher performance, precursors to be utilized in selected materials applications.

Because supersonic beams have the ability to provide precursors with kinetic energies over a wide range, it is an ideal

[†] Part of the special issue "John C. Tully Festschrift".

* To whom correspondence should be addressed. E-mail: s-sibener@uchicago.edu.

[‡] Present Address: Applied Materials, 2727 Augustine Dr. M/S 0770, Santa Clara, California 95054.

10.1021/jp020905u CCC: $22.00 © 2002 American Chemical Society
Published on Web 07/16/2002

technique for studying the effects of incident translational energy on film growth. Early uses of supersonic beams for thin film deposition have taken advantage of the narrow reactant velocity distribution to provide accurate control of trimethylgallium during GaAs homoepitaxy,[4] and the increased beam intensity of such beams to achieve very high epitaxial growth rates of Ge on GaAs.[5] Also worthy of mention is a kinetic study of the reactive conversion of Si(100) by an acetylene beam to form a buffer layer of β-SiC,[6] and the room-temperature growth of silicon nitride from reactive Si and N atoms carried by a sonic jet.[7] Although the only attempt in these early years to actually control the reactant kinetic energy during growth came in a study using translationally hot oxygen atoms for thick oxide layers,[8] numerous groups, including ours, have recently demonstrated the advantages provided by the deliberate control of incident kinetic energy for film growth via supersonic beams. For example, growth of good quality homoepitaxial crystalline Si films at temperatures 200 K lower than the conventional limit was achieved with a high kinetic energy disilane beam.[9] Enhancement of growth rate was seen for aluminum nitride on Si(100) using energized triethylaluminum and ammonia.[10] Growth rate enhancement was likewise seen during homoepitaxial silicon growth with a continuous supersonic disilane beam, although source kinetic energy did not seem to influence film morphology.[11] SiC and GaN have now been grown at reduced temperatures and higher growth rates and structural orientation with supersonic methylsilane and triethylgallium sources.[12,13]

We report here on the deliberate control of reagent kinetic energy as a growth parameter during molecular beam deposition of epitaxial β-SiC on Si(100).[14] We have carried out growth experiments involving the use of two different precursors, hexamethyldisilane $Si_2(CH_3)_6$ and methylsilane $SiH_3(CH_3)$, delivered continuously onto the substrate as seeded supersonic molecular beams. This paper primarily focuses on the methylsilane. Two other groups have also recently examined growth with tetramethylsilane,[16] dimethylethylsilane and methylsilane[12,13,15,17] supersonic beams. Our work was carried out at temperatures some 300 K to 500 K lower than conventional CVD conditions to examine the feasibility of low temperature epitaxial growth utilizing kinetically energetic precursors. We also report dramatic differences in film morphologies and growth behavior as a function of incident kinetic energy. We believe that the methylsilane results reported in ref 17 using 900 C growth temperature overlap the low energy (<0.1 eV) results of our methylsilane work, but they did not characterize nor vary the incident energy of their pulsed beams. Moreover, the fascinating three-dimensional growth features we report here for 0.45 eV beams (down to 930 K) were not observed in the other methylsilane studies even at 0.7−1.4 eV incident energies.[12,13,15] These features are related to those observed in ref 16, with their work using growth temperatures more than 200 degrees higher than those used here and separate but coincident tetramethylsilane $Si(CH_3)_4$ and trisilane Si_3H_8 pulsed beams (again with uncharacterized incident energies).[16]

β-Silicon carbide is a wide band gap compound semiconductor which has viable technological potential for use in high power, high frequency, high temperature, light emitting, and radiation resistant microelectronic devices.[21] Separate precursors, such as silane or disilane and acetylene or propane for silicon and carbon, respectively, are commonly employed in CVD and MBE growth of films for device purposes. A surface carbonization step producing a so-called "buffer layer",[22−23] via the initial reaction of the silicon surface with the carbon-containing gas, reduces the mismatches in thermal expansion coefficients and lattice parameters. Significantly lower growth temperatures are necessary in order to increase the feasibility of device fabrication. Alternative growth techniques, such as the use of single component molecular precursors containing the Si−C moiety, are attractive for lower CVD temperatures.[24] Compounds containing Si−C bonds in the original molecules simplify the reaction system and may be effective for forming Si−C bonds on the surface of growing SiC.

When this work was initiated, we hoped to demonstrate that the use of supersonic beam techniques to deliver such single-source molecular precursors at high incident energies would result in the further lowering of the growth temperature for high-quality β-SiC films. The choice of the precursors methylsilane and hexamethyldisilane was dictated by the ease of attaining hyperthermal energies by the seeded beam method, and by the fact that they were potentially of interest as CVD growth precursors for β-SiC.[24−30] Kinetic studies provided significant insights to the growth mechanisms involved in the methylsilane-based SiC CVD at substrate temperatures as low as 750 C.[24−27] An exponential dependence on the incident methylsilane kinetic energy has been demonstrated for the reaction probability on β-SiC(100).[31] Being a smaller molecular weight precursor, methylsilane is more difficult to deliver than hexamethyldisilane at about 2 eV incident energies as a seeded beam using rare gas carriers. However, methylsilane has another important advantage: it is a stoichiometric CVD precursor with a considerably smaller activation energy than hexamethyldisilane.

Although we observed incident translational energy enhancement of film growth efficiency using either precursor, only methylsilane beams showed dramatic differences in film morphologies and growth behavior with incident energy. The desirable effect of using incident energy to facilitate the initial precursor dissociative chemisorption was achieved for hexamethyldisilane, as inferred from the exponential dependence of growth rate on incident energy between 0.2 eV to 2.8 eV. Despite this, the succeeding growth steps were limited by the reaction of out-diffused silicon atoms from the underlying substrate with the chemisorbed hexamethyldisilane fragments.[14] Growth under high hexamethyldisilane saturation conditions (high incident flux and low substrate temperature) slowed and stopped when films reach a certain thickness. Moreover, hexamethyldisilane incident energy exhibited negligible effect on the quality of the films when compared to the more apparent effect of growth temperature (800−1100 K). Hence, although the hexamethyldisilane chemisorption step was overcome at higher incident energies, the succeeding steps in the growth process solely from the fragment species remained thermodynamically and/or kinetically limited at low temperatures.

In contrast to the (unexciting) hexamethyldisilane behavior, we find that supersonic molecular beam epitaxy (SMBE) growth employing methylsilane on Si(100) can indeed substantially lower the temperature (to about 900 K) at which good films can be grown using moderately high incident energies. Growth at 0.45 eV using solely this precursor was unbounded (continuous and not thickness-limited). This stands in sharp contrast to the previously discussed Si out-diffusion mechanism. Growth proceeded beyond the simple carbonization stage with rate independent of the presence of a buffer layer. In addition to the enhancement of the growth efficiency, square-pyramidally shaped, azimuthally aligned, and spatially isolated three-dimensional features identified as epitaxial Si islands are found to grow simultaneously with two-dimensional SiC film only at higher (0.45 eV) incident energy. These structures are similar to those previously observed at much higher growth tempera-

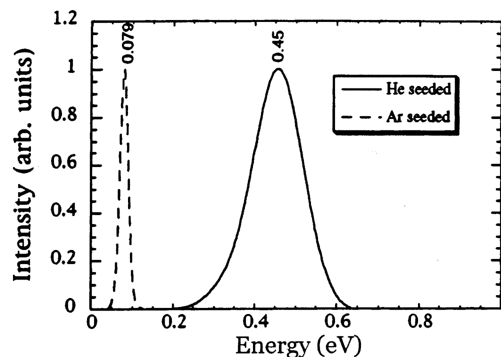

Figure 1. Normalized translational energy distributions of methylsilane beams seeded in helium and argon with the nozzle held at ambient temperature. The mean energy for each distribution appears in the figure.

tures when a separate Si hydride gas-source was employed.[16] We consider the appearance of such features from a single precursor, and only when delivered at the higher energy specifically used in our work, to be a remarkable observation.

II. Experimental Details

Methylsilane (Voltaix) diluted in either helium or argon to 5% concentration was expanded at room temperature using 500−1350 Torr stagnation pressures through a 50 μm pinhole in a differentially pumped chamber. After passing through a skimmer, the supersonic beam struck the Si(100) sample 9 cm downstream from the nozzle inside a UHV chamber. A line-of-sight mass spectrometer allowed for velocity characterization of the beams and ensured that identical on-target methylsilane fluxes were used independent of gas mixture. The respective velocity distributions were well separated in energy, Figure 1, and were independent of the stagnation pressure over the ranges used; two methylsilane flux conditions (ca. 8×10^{14} molecules/cm^2-sec and 1.6×10^{15} molecules/cm^2-sec) where used in these experiments. Beams having higher incident energies than 0.45 eV were not explored as this energy was sufficient to show dramatic differences as compared to lower energy deposition.

Si(100) samples, prepared by standard RCA cleaning procedures, and etched in 1−2% HF solution, were loaded within 15 min after etching into the UHV chamber via a transfer load lock onto a manipulator which allowed the sample's polar angle to be varied with respect to the direction of the incident beam. Consistent with previously reported AFM[32] and STM[33] studies, the ex-situ prepared samples exhibited very flat overall topography with an RMS roughness of about 3−6 Å. Although hydrogen passivated samples prepared in the above manner can have small amounts of O and C contamination,[34] the trace level of residual sample contamination was sufficiently low as to have negligible effect on the experiments. Further in-vacuum thermal treatments carried out prior to deposition likewise did not alter the results.

Deposition of SiC was carried out at substrate temperatures spanning 800−1100 K. The precursor beams were allowed to strike the sample surface at the start of the temperature ramp (>5 K/s) from 800 K to the desired deposition temperature. Background pressures during any temperature ramp prior to SMBE deposition were kept below 3.0×10^{-8} Torr in order to minimize formation of nanometer size SiC crystallites from the background gas. During the actual depositions, the UHV chamber pressure rose to no more than 5×10^{-6} Torr (quoted pressures are for He seeded beams and uncorrected for gas-dependent ionization gauge sensitivities).

A growth area consistent with the estimated beam spot (4 mm diameter) was clearly visible on all samples. A single peak

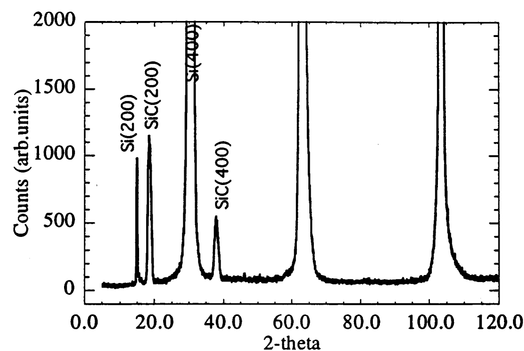

Figure 2. Representative X-ray diffraction $\theta-2\theta$ pattern of epitaxial β-SiC film grown on Si(100) using supersonic beam deposition of methylsilane. The data shown is for a 2000 Å film grown on bare Si at 930 K with 0.45 eV methylsilane, beam flux ca. 1.6×10^{15} molecules/cm^2-sec. Note that the forbidden Si(200) peak for perfectly crystalline Si appears here and is likely due to small crystalline imperfections; it's intensity is at least 500× weaker than the (400) peak. Isolated 3D features identified as epitaxial Si islands (see the discussion) may also contribute to the Si(200) peak.

is seen in the FTIR spectra of all the films grown at substrate temperatures $T_s = 830-1030$ K, with peak position 794−800 cm^{-1} corresponding to the known Si−C stretching vibration, and width (fwhm = 25−50 cm^{-1}) being characteristic of crystalline SiC.[35] Film thicknesses were extracted from the SiC IR transmission peak, which can be related to the relative amount of carbon in the films via classical dispersion theory.[35] X-ray $\theta/2\theta$ diffraction (Mo$K\alpha$ radiation with $\lambda = 0.71069$ Å) of all the films confirm the SiC phase obtained was purely cubic and epitaxial with respect to the Si(100) substrate (Figure 2). Quantitative use of the diffraction peak widths (fwhm's) of either the $\theta/2\theta$ diffraction peaks or ω rocking curves was complicated by the large instrument function (spatial dispersion) of the diffractometer employed. Select samples showed variations in peak widths of 0.5−0.6° for the rocking curves around the SiC (200) peak, whereas the rocking curve around the huge substrate (400) peak was narrower, with 0.25° fwhm. Thus, qualitative but not quantitative conclusions about relative crystalline quality could be drawn from the observed changes in measured peak widths. Ex-situ scanning force and electron microscopies were used for morphological characterization of the grown films. Spatially resolved compositional assignment of relevant growth features was further accomplished using high spatial resolution and element specific SIMS imaging.

III. Results

A. Incident Translational Energy Effects on Film Growth Efficiency and Growth Behavior. Figure 3 compares the efficiencies for film growth with 79 and 450 meV methylsilane at three different deposition conditions (different combinations of incident flux and substrate temperature). The growth efficiency is defined as the ratio of the amount of deposited carbide to that observed if each carbon atom in an incident precursor molecule led to a SiC unit. The growth efficiency at the higher incident energy is about 10 times enhanced, yet the incident energy is only about 20−30% of the thermal activation energy found for CVD growth (1.8−2.2 eV). The growth efficiencies reported for low-pressure CVD are about 5×10^{-5} at 930 K, 5×10^{-4} at 1030 K, and 3×10^{-2} at 1273 K.[26,27] (The reaction probability of methylsilane on a β-SiC(100) surface at 1220 K, as recently measured by modulated molecular beam reflectivity, is approximately 0.02 at 800 meV incident energy.[31])

Figure 4 shows that the β-SiC film thickness grows linearly (20 Å/min) with deposition period at Ts = 930 K for the 0.45

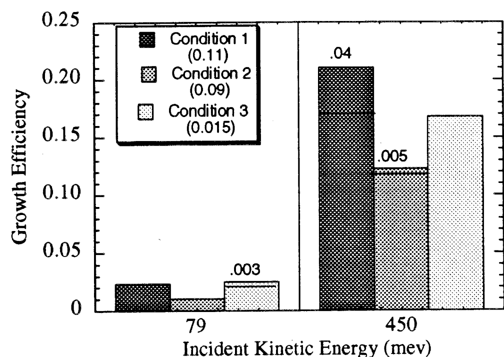

Figure 3. Film growth efficiency at various deposition conditions for 0.079 and 0.45 eV methylsilane incident translational energies. The numbers 0.11, 0.09, and 0.15 parenthetically enclosed for each condition is the ratio of the efficiency at the lower energy to that at the higher. The deposition conditions are (1) T_s = 930 K, methylsilane flux ca. 1.6×10^{15} molecules/cm^2-sec; (2) T_s = 1030 K, methylsilane flux ca. 1.6×10^{15} molecules/cm^2-sec; and (3) T_s = 930 K, methylsilane flux ca. 0.8×10^{15} molecules/cm^2-sec. Error magnitudes are indicated on top of each growth efficiency bar.

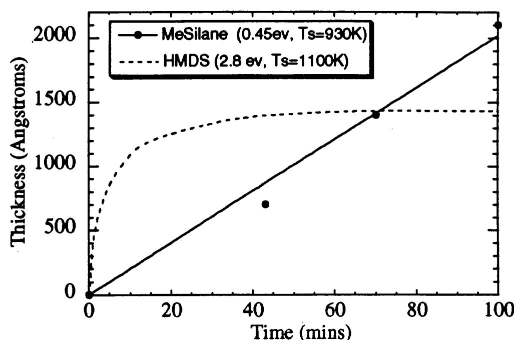

Figure 4. Evolution of film thickness during growth at T_s = 930 K using 0.45 eV higher flux methylsilane (ca. 1.6×10^{15} molecules/cm^2-sec). Shown for comparison is the curve for growth using 2.8 eV hexamethyldisilane at the same flux (ref 13).

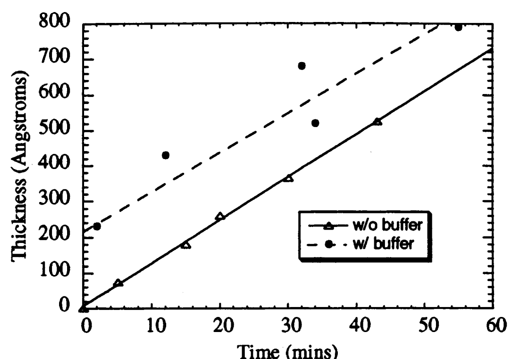

Figure 5. Evolution of film thickness during growth at T_s = 1030 K on bare Si(100) and on top of a buffer (carbonized surface) layer. Methylsilane beam conditions as in Figure 4.

eV beam. This growth rate is comparable to those reported at 870−970 K using 0.7 eV beams of about the same flux.[12] Additionally, growth does not saturate. This differs markedly from the mechanism using out-diffused Si as seen with (a) hexamethyldisilane up to 2 eV,[14] (b) carbon only (C_2H_2) beams[6] and (c) the low energy pulsed methylsilane beam where growth ceases at 500 Å.[17] This unbounded growth is likewise shown for T_s = 1030 K in Figure 5 where growth on top of a β-SiC buffer layer proceeds at a similar rate (12 Å/min) as on a bare substrate. The buffer layer, which is a 200 Å film grown through the reactive conversion of the silicon surface with acetylene (i.e., via silicon atom out-diffusion),[22,23] was observed to be covered with hillocks (oval shaped defects) on the surface, and riddled with substrate etch pits (from the consumption of substrate Si in the carbonization process). Further growth on top of this buffer layer with either acetylene, low energy methylsilane (<0.1 eV), or 2 eV hexamethyldisilane does not occur. Whether or not a buffer layer exists is therefore unimportant for the present case of energetic 0.45 eV methylsilane, i.e., film growth clearly depends solely on the supply of methylsilane at the right energy.

The film growth rate when using an incident angle of 60° is roughly 5 times less than that for a normal incidence. (Note that the necessary correction for the dependence of beam flux with polar angle, i.e., the flux of molecules impinging onto the surface is proportional to cosine of the incident angle, was properly taken into account.) This angular dependence reflects the dependence of the growth efficiency on the scaled normal component of incident energy $E_{tot} \cos^n\theta$, $n = 0.3$ for methylsilane on β-SiC(100).[31] This scaled energy dependence was similarly inferred by Ustin et al.[12] based on the slight negative temperature dependence of methylsilane growth at incident energies above 0.5 eV caused by the roughness increase with growth temperature; we likewise observe this negative temperature dependence at 0.45 eV as shown in Section C below. (We have also observed such a scaled energy dependence for growth efficiency when using hexamethyldisilane, and compared our results to the reaction probability of its analogue disilane studied via modulated molecular beam reflectivity;[14,36] these results will be reported elsewhere.)

B. Growth Morphology and Film Evolution versus Incident Kinetic Energy. The film morphologies obtained at the three deposition conditions (different combinations of incident flux and substrate temperature corresponding to Figure 3 above) display attributes that reflect the incident methylsilane energy employed. Figure 6a,b contains images representative of films grown at the lower and higher incident energies, respectively. The films obtained at the low incident energy are all characterized by the presence of pits and substrate etch pits (intense dark square features) and 50−200 nm square-based grains. These films clearly consist of crystallites with well defined and high angle grain boundaries. This observed morphology for low energy growth is identical to the observations reported for the pulsed methylsilane beams of unknown but presumably low energy in ref 17. Taken together with the thickness-limited growth behavior mentioned in Part A above, the films generated with low incident energy methylsilane are epitaxial β-SiC grown by the reaction of silicon atoms out-diffused from the substrate with surface-bound carbon-containing species from methylsilane. This growth mechanism occurs during buffer layer formation, as well as for growth involving hexamethyldisilane even at 2 eV energies.[14,22] On the other hand, for high incident energy methylsilane, the films produced exhibit sparse isolated micron size three-dimensional granular features on an otherwise relatively smooth, continuous and void-free film. Unlike the films grown at lower methylsilane energy (this work and ref 17) or using hexamethyldisilane up to 2 eV,[14] the 450 meV films do not show the dark contrast markings of the substrate etch pits. Moreover, the isolated three-dimensional features are often square-pyramidal in shape, facetted, and azimuthally aligned with respect to the substrate.

Figure 7 contains representative force microscopy images of films grown with 0.45 eV at T_s = 1030 K on bare Si and on a buffer layer. The figures are presented in an illuminated perspective view with shadows for contrast enhancement to

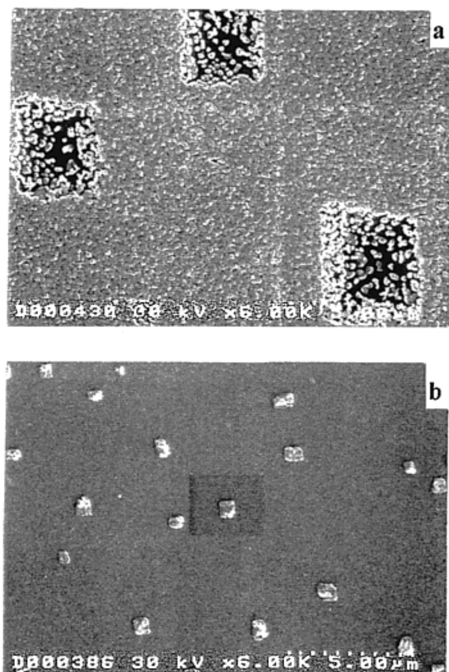

Figure 6. Representative SEM images of films grown using methylsilane of incident energy (a) 0.079 eV and (b) 0.45 eV. The scale bars are both 5 microns. The dark square patch in the middle of (b) is an artifact due to e-beam damage from magnification and is unrelated to the relevant intense dark square pits of (a).

show simultaneously the isolated 3-dimensional features and the surrounding material. The material around the isolated 3-dimensional features exhibits the doubly degenerate domain structure of the cubic (100) surface. In the absence of high-resolution XRD line width or rocking curve data, it is not possible to quantify the mosaic spread of the highly oriented crystallites which likely comprise the film (i.e. the film is not expected to be monocrystalline, as is typical of most heteroepitaxial films due to the lattice mismatch between substrate and overlayer.[37]) However, the crystallites are clearly highly textured with very low angle boundaries such that the overall morphology is improved over films grown at lower energy. Note also that the rms roughness of the material is 2.5−3.0 nm, smoother than the films obtained from either hexamethyldisilane or low energy methylsilane (for comparable film thickness, 4−10 nm rms roughness). Furthermore, it is more compact and void free. It is therefore like a “two-dimensional wetting layer” and will be referred to as “2D layer”, but only to distinguish it from the film obtained at lower energy and from the isolated 3D features. It may be noted that the best quality films grown by conventional CVD from methylsilane also have considerable surface roughness, with surface features of lateral dimensions 0.1−0.2 μm being observed.[25]

From either Figure 7 or the wider scan images shown in Figure 8 (from which Figures 7 were magnified), it is seen that the isolated 3-dimensional features are square shaped and azimuthally aligned, sometimes pyramidal and facetted, and occasionally have smooth tops—implying that these are epitaxial cubic structures. Spatially resolved and element-specific SIMS analysis of the 3D island composition, shown in Figure 9, indicates that the well-faceted islands are Si and not SiC. Similar islands on SiC films, grown on Si(100) employing two pulsed beams containing trisilane (minimal concentration) and $Si(CH_3)_4$, have been assigned as epitaxial Si using transmission electron diffraction.[16] Two other groups have also reported Si island formation on 6H−SiC substrates employing either physical

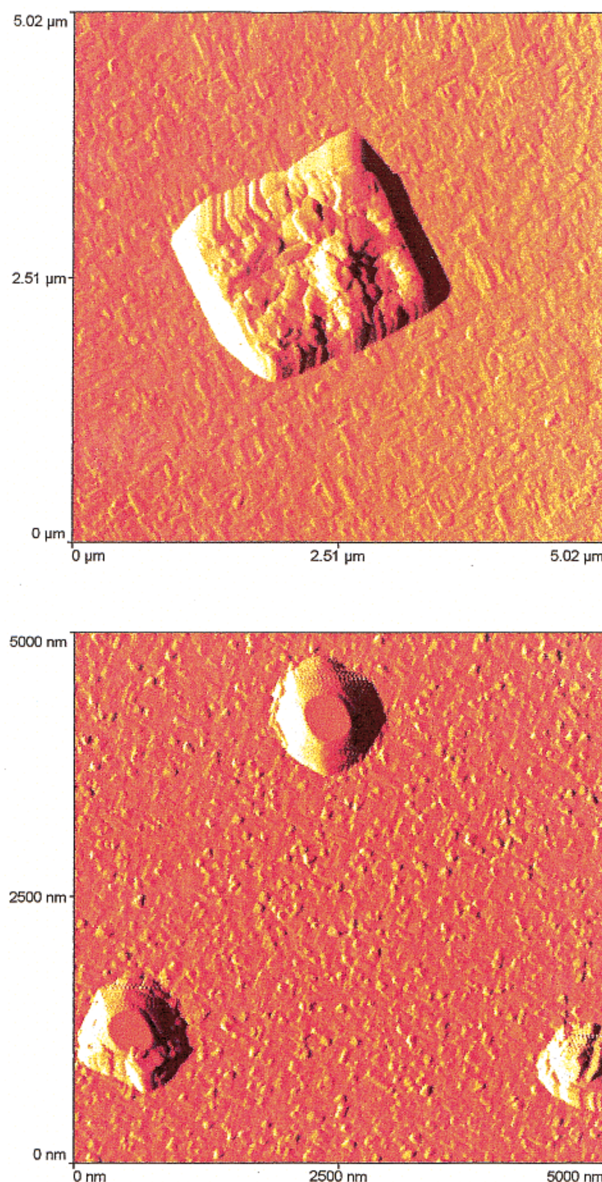

Figure 7. Representative scanning force microscopy images of films grown at T_s = 1030 K using 0.45 eV higher flux methylsilane. The data shown are for growth on bare Si 43 min duration (bottom image) and on top of a buffer layer 53 min duration (top image). The 5 × 5 μm scans are presented in illuminated perspective views with shadow effect for contrast enhancement to show simultaneously the isolated 3-dimensional features and the structure of the surrounding material.

evaporation of Si on 800 K−900 K substrates or with alternating exposures of disilane and acetylene on 1100 K substrates.[38,39] Energetic methylsilane up to 1.4 eV using hydrogen carrier on the other hand may not have produced such islands since hydrogen pushes the equilibria toward Si evaporation.[13,15,40] Furthermore, when separate supplies of Si (trisilane[16] or disilane[39]) are used for growth either on Si or 6H−SiC substrate, the island densities are seen to depend on the relative intensity of the Si source to the carbon source. Thus, our observations at higher incident energies indicate that Si from methylsilane becomes more efficiently incorporated into the growing film so that quantities exist in excess of that required to support growth of the stoichiometric SiC film. This excess Si precipitates out and forms the epitaxial 3D islands. Of course, as these islands get bigger, carbidization of the island surfaces is possible. This has in fact already been reported for the Si islands observed on 6H−SiC[39] and indicated by a minority number of islands

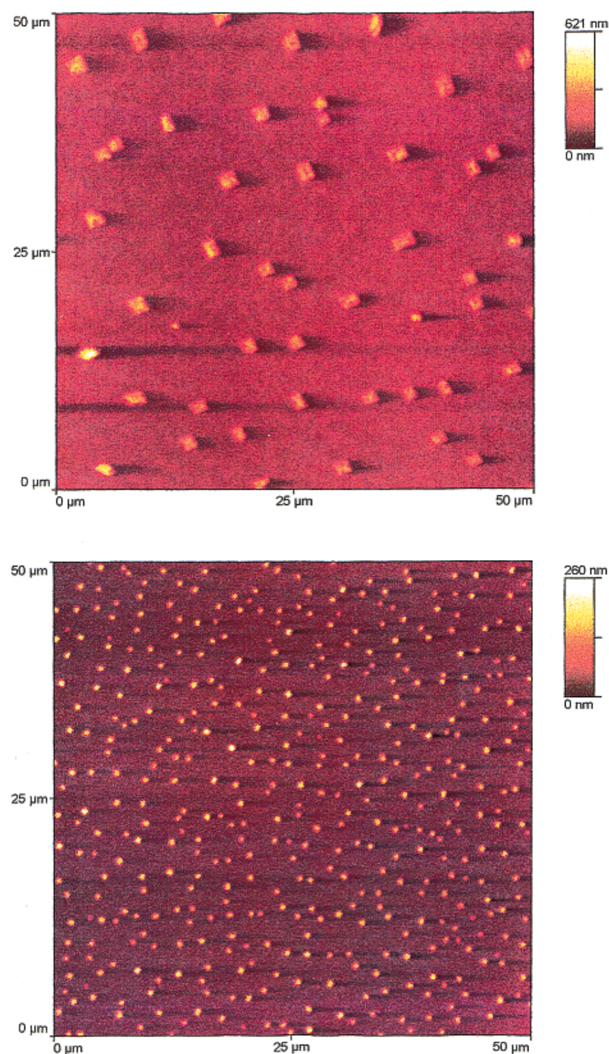

Figure 8. 50 × 50 μm scannning force microscopy images of the same films shown in Figure 7.

having minimal carbon signal in the imaging SIMS data of Figure 9. Overall, it is clear from our observations that high incident energy deposition has opened up a new growth behavior from a single-source precursor, as evidenced by these new 3D Si features as well as by the epitaxial β-SiC 2D layer of improved quality. This channel was not observed with energetic hexamethyldisilane[14] or low energy methylsilane, regardless of substrate temperature or incident flux.

Figure 10 is a wide scan image of the film obtained at lower temperature, 930 K, which shows that both the 3D Si island density (ca. 10^6-10^7/cm^2) and their size distribution depend on growth temperature (compare with Figure 8 bottom image). A careful analysis of the density and size distribution for various deposition periods and temperature may be useful in understanding their origin, but will be reported elsewhere. In the meantime, while providing information on the nature of the growth process, some insights about the occurrence of the 3D Si islands may also be gained from examining film evolution during growth.

The film morphology at early times for $T_s = 1030$ K can be characterized by the presence of pits, Figure 11a. After a transition period where both pits and 3D Si islands exist, Figure 11b, only the smooth void-free 2D SiC layer is seen together with the 3D Si islands, Figure 11c. The 3D island density and size increased with deposition time (to be discussed elsewhere). The morphological evolution for the film grown on top of the

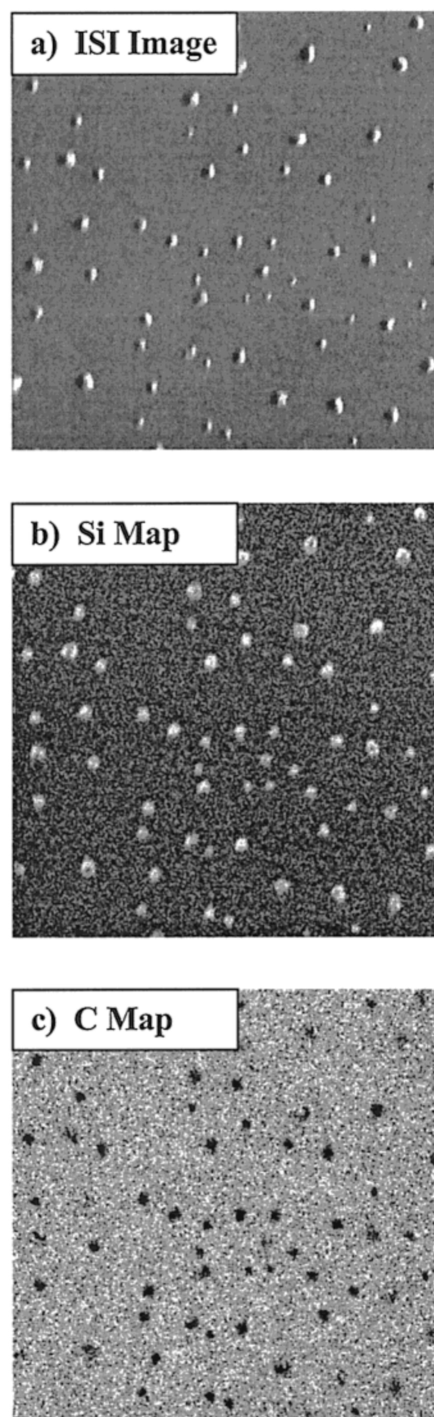

Figure 9. Spatially resolved composition analysis using element-specific SIMS imaging: (a) Ion-induced secondary ion (ISI) topographic image which shows the 2D and 3D stuctures *without* element-specific mass resolution (b) Si map which confirms that the 3D islands (bright regions) and 2D layer both contain Si; (c) C map which indicates that C is absent at the 3D island locations (dark regions) while present in the 2D layer.

buffer layer (pre-grown with C_2H_2) behaves similarly. Initially, the 3D Si islands are nucleated on the hillock-covered buffer layer, Figure 12a. As the 3D Si islands grow in size, Figure 12b, the 2D SiC layer grows on top of the buffer layer and eventually covers the hillocks, Figure 12c. It may be noted that the dark contrast features marking the substrate etch pits formed earlier during the buffer layer growth do not increase in size when additional film is grown with the energetic 0.45 eV methylsilane. This is in contrast to the case for low energy

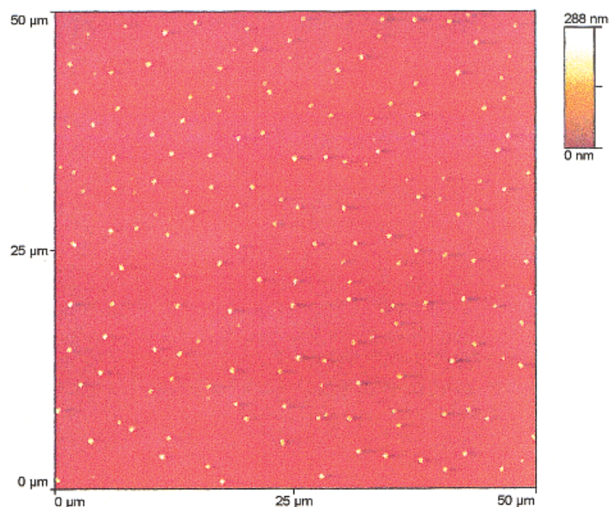

Figure 10. 50 μm scanning force microscopy image of a film grown at T_s = 930 K on bare Si and the same beam condition and deposition period as the bottom image shown in Figure 8.

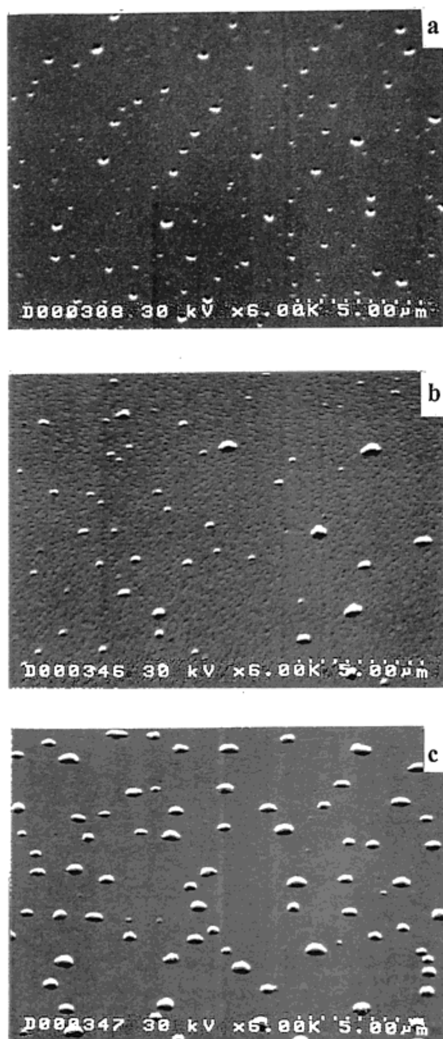

Figure 11. Off-normal SEM images of films grown at T_s = 1030 K with 0.45 eV higher flux methylsilane on bare Si(100) for progressively longer periods: (a) 5 min, 75 Å; (b) 20 min, 260 Å; and (c) 43 min, 525 Å.

methylsilane and hexamethyldisilane, and supports the conclusion that film growth at the higher incident energy is not through the mechanism involving out-diffused silicon atoms.

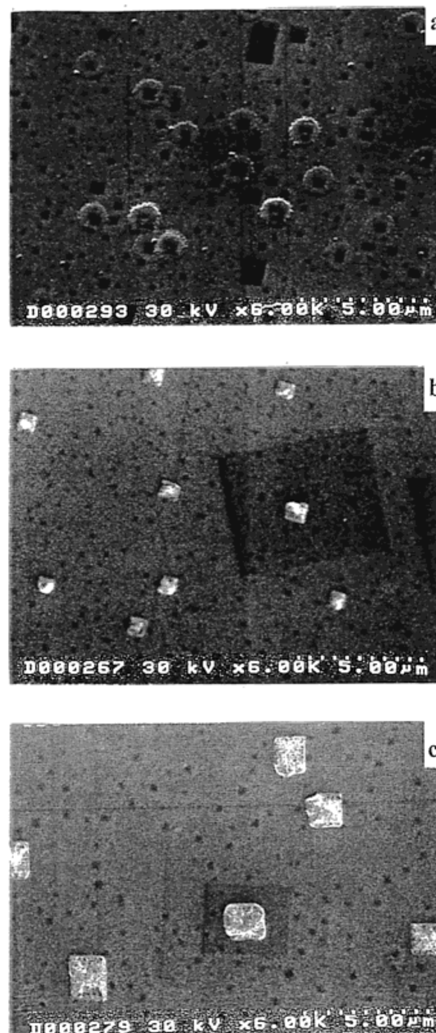

Figure 12. Off-normal SEM images of films grown at T_s = 1030 K with 0.45 eV higher flux methylsilane on top of a 200 Å buffer layer for progressively longer periods: (a) 10 min, total thickness = 430 Å; (b) 30 min, 520 Å; and (c) 53 min, 790 Å. The intense dark contrast features in (a) which appear smaller in (b) and (c) as the film thickens are the relevant substrate etch pits, while the large dark square regions in (b) & (c) are artifacts due to e-beam damage.

The growth of the 3D epitaxial Si islands on the buffer layer at high incident energies is remarkable. For the case of the trisilane pulsed beam added to tetramethylsilane for SiC growth on bare Si, islands were evidently nucleated at pits as the interfacial SiC layer grew.[16] Si from the trisilane continuously diffused to this pit locations to grow the nucleated islands further. However, when a buffer layer is pre-grown, as done in our work, the pits get buried and closed off, and the locations of the 3D islands appear to have no relation to the pit locations underneath the buffer layer. Thus, at higher incident energies, excess Si from methylsilane forms the epitaxial 3D islands everywhere on the epitaxial SiC layer. This Si islanding may serve as an indicator for the quality of the 2D SiC layer, and will be exploited in the next section to help find the minimum temperature at which epitaxial β-SiC can be grown at 0.45 eV energy.

It has already been suggested by the above observations that the 2D SiC layer and the 3D Si islands grow simultaneously. The data shown in the images of Figure 13 corroborate this observation. After a film is intentionally deposited using a high energy methysilane beam at normal incidence for 43 min, Figure 13a, it is then exposed to further deposition for 57 min with

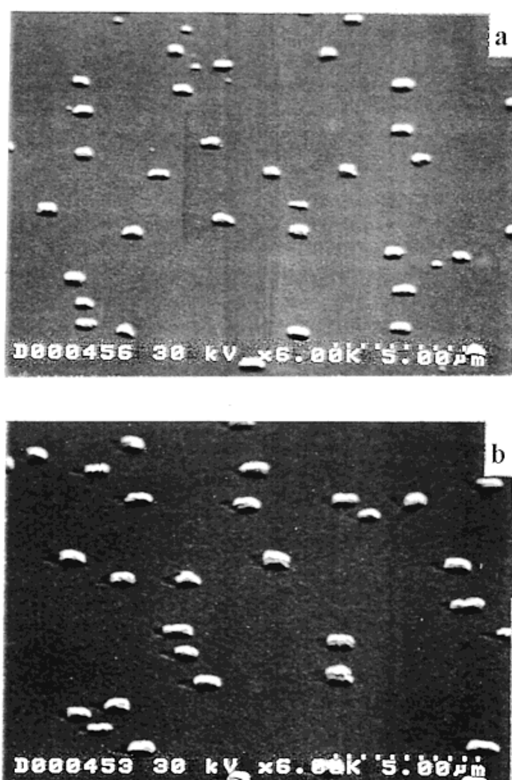

Figure 13. Off-normal SEM images of a film grown at $T_s = 930$ K using 0.45 eV higher flux methylsilane after (a) 43 min of initial deposition at normal incidence, and (b) a subsequent additional 57 min of glancing angle deposition at 60° incidence with respect to the surface normal with the incident beam impinging from the right side of the image. Note the clearly resolved "downstream" shadows cast by the micron-sized Si islands, as well as the relatively tight size distribution of the Si islands.

the beam striking the surface at 60 degrees from the surface normal, Figure 13b. The 3D islands cast clear shadows on the far (downstream) side from the incident beam direction, while the islands themselves continue to grow in size during the glancing angle deposition ("GLAD"). Note that no such shadows are seen for deposition at normal incidence (the deposition condition used for all the films discussed before this point). The cast shadows during GLAD are roughly triangular, as would be expected from pyramidal 3D Si islands. The occurrence of the shadows implies that the 2D SiC layer grew simultaneously with the 3D islands. This also demonstrates that a clear advantage of beam deposition over CVD is the ability to control the directionality of the incident flux and, hence, influence the growth morphology.

A force microscopy image of the shadows next to the islands is shown in Figure 14. From line scan analysis, we see that the 2D SiC layer grew at a rate of approximately 3 Å/min (T_s = 930 K). Noting that there are 1.05×10^{15} SiC units in a unit volume of β-SiC bounded by 2 layers (interlayer spacing = 1.089 Å) and 1 cm^2 area, this growth rate is equivalent to 5×10^{13} SiC units/sec. Likewise, from analysis of wide scan force microscopy images of the islands, the increase in total island volume in a 1 cm^2 area is approximately 2×10^3 μm^3/min, or, equivalently, 1×10^{13} Si units/sec (Si 100 interlayer spacing = 1.36 Å). We therefore see that growth on the 2D layer accounts for most of the growth of the film, being about 5 times larger on a volume basis than on the 3D islands, i.e., the majority of volume growth is generated by 2D SiC layers as opposed to the sparse 3D Si islands.

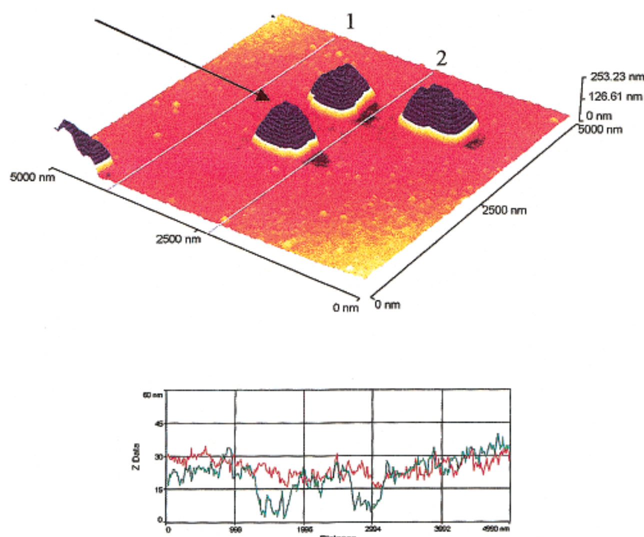

Figure 14. Scanning force microscopy image of the film shown in Figure 12b. Surface profiles along the indicated lines are also plotted with the bottom trace corresponding to line #2 (passing through the shadows). The direction of the incident precursor beam is indicated by the arrow.

C. Decreased Threshold Growth Temperature With Higher-Energy SMBE. This is a system that offers a superb test case for exploring whether translational energy can be used as a control parameter for decreasing the threshold temperature needed for growth of epitaxial β-SiC. Continuous film growth, which depends solely on the incident energy of the precursor, has already been demonstrated at Ts = 930 K. This is about 70 to 100 degrees lower than the previously reported onset temperature for CVD growth using the same precursor, yet the incident energy used is still only 20−30% of the CVD thermal activation energy.[24−26] With this incident energy, it is of further interest to uncover the lowest possible growth temperature.

Films produced below T_s = 900 K exhibit rough morphologies with no signs of isolated 3D islands (Figure 15). While these films also exhibit the epitaxial β-SiC X-ray diffraction peaks, in the absence of comparative XRD FWHM, the quality of these films can only be judged by the absence of the epitaxial 3D islands. That is, films grown below 900 K are of inferior quality than those above 900 K based on the fact that they do not serve as template layers for the well-facetted and aligned Si islands. It should also be noted that Si islanding occurs on well-defined SiC substrates even below 900 K when using Si physical vapor deposition,[38] as well as for low-pressure CVD when using silicon hydrides with substrate temperatures down to ca. 830 K.[40]Additionally, film thickness evolution, when plotted as a function of growth temperature, Figure 16, cannot be fit satisfactorily by a single linear curve. It is perhaps not coincidental that T_s = 900 K appears to be a point where a break in slope occurs, suggesting that the data can be naturally divided into two growth temperature regimes. That is, films grown above T_s = 900 K, having identical morphologies (as described in the previous section), show a negative temperature dependence of their growth rates which can be linearly fit with minimal scatter. On the other hand, films grown below this temperature, exhibiting drastically different morphologies, have a linear fit of the film thicknesses with considerably larger scatter, with the films displaying rougher morphologies (Figure 15a for films grown at T_s = 855 and 880 K) having positive deviation from the fit while those of lesser roughness (Figure 15b for T_s = 830 and 890 K) having negative deviation. The clearest observation is that the morphologies of the films grown

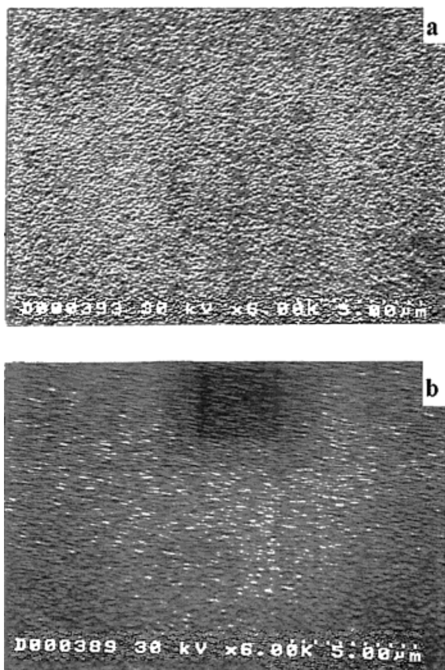

Figure 15. Off-normal SEM images of films grown with 0.45 eV higher flux methylsilane for 43 min at substrate temperatures below 900 K: (a) 880 K, 1450 Å; and (b) 830 K, 1350 Å.

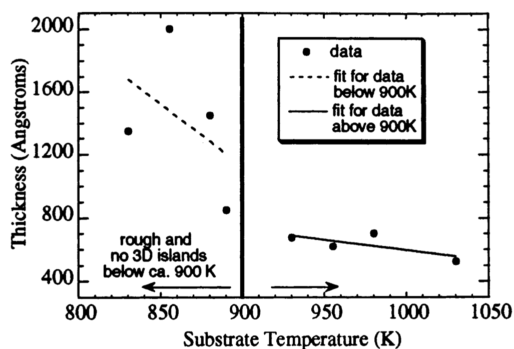

Figure 16. Thickness (or growth rate, 43 min deposition time) vs Substrate Temperature using 0.45 eV methylsilane. Division of data into two substrate temperature controlled growth regimes is suggested by observed film morphologies (see text).

above and below 900 K differ markedly; we infer from this that the onset growth temperature for epitaxial β-SiC when using 450 meV methylsilane is ca. 900 K.

IV. Discussion and Conclusion

The results reported herein clearly demonstrate the significance of incident translational energy in low-temperature epitaxial β-SiC film growth. In addition to growth efficiency enhancement, successful film growth at temperatures lower than those used in conventional CVD processes was clearly achieved. This suggests an operative growth mechanism at high incident energies that is not present at lower energies.

A picture of the growth process at low temperatures is as follows: film growth from low energy methylsilane is no different from that for hexamethyldisilane or a pure hydrocarbon where out-diffused silicon atoms react with both physisorbed and dissociatively adsorbed methylsilane. Although methylsilane is a stoichiometric precursor, this is the preferred pathway because Si from methylsilane is apparently not delivered to or incorporated into the growing film with the same efficiency as carbon. On the other hand, at high incident energies a second growth mechanism exists in addition to that present at low incident energy. This second growth mechanism takes over from the silicon atom based mechanism as the out-diffusion of substrate silicon slows with increasing film thickness. This becomes possible at high energies because Si from methylsilane is at a minimum just as efficiently delivered or incorporated as carbon. (Si deposition may even be more efficient than that for C given that excess Si is available for island precipitation and simultaneous SiC film growth.) Thus, this second growth mechanism allows film growth to proceed continuously when the first mechanism becomes essentially inoperative (due to either increased film thickness or intentionally made inoperative due to the presence of an initial buffer layer). It is also important to note that this second mechanism occurs simultaneously with the first (silicon atom based) mechanism. This prevents the formation of the oval shaped hillocks characteristic of the insufficient supply of Si from the substrate (as in the case of acetylene and hexamethyldisilane grown SiC films) when silicon atom out-diffusion slows down. The significance of the silicon atom based mechanism however must not be overlooked. It serves to form an initially pitted film much like the buffer layer which relaxes the lattice mismatch between the silicon substrate and the subsequent film growing via the second mechanism. In summary, we find that a continuously growing epitaxial film of reasonable quality can be obtained, even at relatively low substrate temperatures, when one uses kinetically accelerated methylsilane as the growth precursor.

Recent work on the incident energy dependence of methylsilane reaction probability on β-SiC(100) reported an exponential dependence on the scaled normal component of the incident kinetic energy.[31] A study of the kinetics of CVD growth from methylsilane also points out that the rate determining step is the decomposition of a surface-bound precursor or a physisorbed state of methylsilane.[26] The resulting radicals from the eventual dissociative chemisorption of the precursor are thought to insert subsequently into the Si−H or C−H bonds on the surface forming SiC. This suggests that the effect of incident energy during the supersonic beam deposition of SiC from methylsilane likely results from collisionally activated precursor dissociation. As the primary product in the homogeneous gas-phase decomposition of methylsilane is the methylsilyl radical $HSiCH_3$ (98% yield at 973 K) with an activation energy close to that found for the SiC CVD growth,[41,42] the relevant radical formed from the surface bound methylsilane during CVD growth is also suspected to be $HSiCH_3$.[26] It is tempting to speculate that the second growth mechanism opened up at high methylsilane incident energies is due to these radicals produced by the collisional impact of methylsilane.

Although the second growth mechanism at high incident energies may be attributed to the more abundant supply of methylsilyl or similar radicals, the more complex effect of overcoming thermodynamic and/or kinetic barriers of not only the chemisorption step but also the succeeding growth steps must also be considered. Bond cleavage and rearrangement reactions (after dissociative chemisorption) leading to the insertion of both Si and carbon to the growing film may become more facile, and more balanced between carbon and Si, at high incident energies. Considering that the energy used was only 20−30% of the CVD activation energy, it is possible that vibrational excitation of surface bonds or other lower energy pathways can be accessed even at moderately higher incident energies. It has even been suggested that surface decomposition and incorporation might be concerted, proceeding directly from an activated form of the parent precursor molecule.[26] This was based on the observation that CVD growth using silacyclobutane and methylsilane showed significant structural differences,

indicating participation of different growth species, despite the respective radicals produced upon dissociative chemisorption are isomeric $HSiCH_3$ and $H_2Si{=}CH_2$.

That epitaxial 3D islands of Si are produced on the 200 Å buffer layer from the single precursor methylsilane at 0.45 eV and not at lower energy is rather remarkable. How these islands nucleate and grow is a subject that will be addressed in detail in another report, but will be briefly mentioned here. A statistical analysis of the 3D Si island density and size distribution on our films show that smaller mean island sizes are observed at higher island densities.[14] A further general visual observation is that the islands are not uniformly distributed on the growing film so that distances between nearest neighbor islands are not uniform. Meanwhile, from the mean lateral growth rate of the Si islands, a diffusion length for the Si bearing species ($Si{-}H_x$ fragments if not atomic Si) is calculated to be approximately 0.3 micron at 930 K−1030 K. This is of the same order of magnitude as the typical lateral dimensions of surface features in good quality films from methylsilane CVD.[25] Furthermore, groups of islands in linear arrangement are occasionally observed. The possibility that the film consists of a mosaic of crystallites with low angle boundaries might favor high step densities. With these considered, we suggest the occurrence of preferential Si island nucleation at steps and defects of the growing SiC film once excess Si (or Si bearing species) becomes available. The unknown step and defect distribution on the growing SiC film may be reflected in the Si island distribution. Despite these steps and defects however, the SiC layer must still be of sufficiently high surface quality as to provide a template for epitaxial Si island growth. The top Si layer of Si/β-SiC/Si heterostructures for instance is either epitaxial or randomly oriented polycrystalline, depending on the smoothness and thickness of the β-SiC layer.[43]

The above postulated picture of Si islanding follows the simpler case of physical evaporation of Si on 6H−SiC.[38] In that study, the strong influence of kinetics (Si arrival rate and temperature) on island formation is seen. Well organized arrays of Si islands are also obtained on a stepped (off-oriented) substrate as opposed to random arrangement on flat substrates. Si adatom migration length in the range of 1 micron at 900 K was inferred from the preferential nucleation at the step edges when step distances were less than 1 micron. Such high mobility of Si was attributed to the low migration barrier on SiC. The diffusion length we calculated is therefore reasonable considering that the Si bearing species in the island growth may well be some $Si{-}H_x$ fragments instead of only atomic Si.

To conclude, this combined supersonic molecular beam epitaxy and scanning probe imaging study has definitively shown that the onset temperature for the growth of epitaxial β-SiC can be substantially lowered when using translationally accelerated methylsilane as the growth precursor. Moreover, the deliberate control of incident reagent kinetic energy ensured that the reactive species were supplied in an activated manner that precluded the initial dissociative chemisorption step from being either thermodynamically or kinetically rate limiting at the employed low deposition temperatures. This work merits substantial reflection as it shows, in essence, that the morphology of reactively deposited thin films can indeed be influenced by the initial state of the reactive precursor, suggesting opportunities for film growth at more highly optimized conditions than can be routinely achieved with thermal CVD-type processes.

Acknowledgment. We would like to thank Mark Viste and Nabil Isa for their assistance in beam characterization and force microscopy imaging, and Professor Riccardo Levi-Setti for the element-specific SIMS images of Figure 9. This work was supported by seed funding from the National Science Foundation's Materials Research Science and Engineering Center at the University of Chicago. Microscopy instrumentation funded by the Air Force Office of Scientific Research is also gratefully acknowledged.

References and Notes

(1) Barker, J. A.; Auerbach, D. J. *Surf. Sci. Rep*. **1984**, *4*, 1.
(2) Arumainayagam, C. R.; Madix, R. J. *Prog. Surf. Sci*. **1991**, *38*, 1.
(3) Yu, M. L.; DeLouise, L. A. *Surf. Sci. Rep*. **1994**, *19*, 285.
(4) Zhang, S.; Cui, J.; Tanaka, A.; Aoyagi, Y. *Appl. Phys. Lett.* **1994**, *64*, 1105.
(5) Eres, D.; Lowndes, D. H.; Tischler, J. Z. *Appl. Phys. Lett.* **1989**, *55*, 1008.
(6) Kusunoki, I.; Hiroi, M.; Sato, T.; Igari, Y.; Tomoda, S. *Appl. Surf. Sci.* **1990**, *45*, 171.
(7) Wang, D.; Ma, T. P.; Golz, J. W.; Halpern, B. L.; Schmitt, J. J. *IEEE Electron Device Lett*. **1992**, *13*, 482.
(8) Cross, J. B.; Hoffbauer, M. A.; Farr, J. D.; Glembocki, O. J.; Bermudez, V. M. *Mater. Res. Soc. Symp. Proc*. **1991**, *204*, 59.
(9) Malik, R.; Gulari, E.; Li, S. H.; Bhattacharya, P. K.; Singh, J. *J. Crystal Growth* **1995**, *150*, 984.
(10) Brown, K. A.; Ustin, S. A.; Lauhon, L.; Ho, W. *J. Appl. Phys*. **1996**, *79*, 7667.
(11) Pacheco, K. A.; Ferguson, B. A.; Banerjee, S.; Mullins, C. B. *Appl. Phys. Lett*. **1996**, *69*, 1110.
(12) Ustin, S.; Brown, K.; Ho, W. *Rev. Sci. Instr*. **2000**, *71*, 1479.
(13) Boo, J. H.; Ustin, S.; Ho, W. *Thin Solid Films* **1999**, *343−344*, 650.
(14) Sanchez, E. C. Doctoral Dissertation, University of Chicago, 1997.
(15) Ustin, S.; Long, C.; Ho, W. *Solid-State Electron*. **1998**, *42*, 2321.
(16) Ikoma, Y.; Endo, T.; Watanabe, F.; Motooka, T. *J. Vac. Sci. Technol. A* **1998**, *16*, 763.
(17) Ikoma, Y.; Endo, T.; Watanabe, F.; Motooka, T. *Jpn. J. Appl. Phys. Part 2* **1999**, *38*, L301.
(18) Capano, M. A. *J. Appl. Phys*. **1995**, *78*, 4790.
(19) Knowles, M. P.; Leone, S. R. *Chem. Phys. Lett.* **1996**, *258*, 217.
(20) Eaglesham, D. J. *J. Appl. Phys*. **1995**, *77*, 3597.
(21) Davis, R. F.; Palmour, J. W.; Edmond, J. A. *Diamond Relat. Mater.* **1992**, *1*, 109.
(22) Nishino, S.; Powell, J. A.; Will, H. A. *Appl. Phys. Lett*. **1983**, *42*, 460.
(23) Addamiano, A.; Sprague, J. A. *Appl. Phys. Lett*. **1984**, *44*, 525.
(24) Golecki, I.; Reidinger, F.; Marti, J. *Appl. Phys. Lett*. **1992**, *60*, 1703.
(25) Krotz, G.; Legner, W.; Muller, G.; Grueninger, H. W.; Smith, L.; Leese, B.; Jones, A.; Rushworth, S. *Materials Sci. and Eng*. **1995**, *B29*, 154.
(26) Johnson, D.; Perrin, J.; Mucha, J. A.; Ibbotson, D. E. *J. Phys. Chem.* **1993**, *97*, 12 937.
(27) Ohshita, Y. *J. Cryst. Growth* **1995**, *147*, 111.
(28) Nordell, N.; Nishino, S.; Yang, J. W.; Jacob, C.; Pirouz, P. J. *Electrochem. Soc*. **1995**, *142*, 565.
(29) Nordell, N.; Nishino, S.; Yang, J. W.; Jacob, C.; Pirouz, P. *Appl. Phys. Lett*. **1994**, *64*, 1647.
(30) Chiu, H. T.; Hsu, J. S. *Thin Solid Films* **1994**, *252*, 13.
(31) Xia, L. Q.; Jones, M. E.; Maity, N.; Engstrom, J. R. *J. Vac. Sci. Technol. A* **1995**, *13*, 2651.
(32) Montgomery, J. S.; Schneider, T. P.; Carter, R. J.; Barnak, J. P.; Chen, Y. L.; Hauser, J. R.; Nemanich, R. J. *Appl. Phys. Lett.* **1995**, *67*, 2194.
(33) Neuwald, U.; Hessel, H. E.; Feltz, A.; Memmert, U.; Behm, R. J. *Surf. Sci*. **1993**, *296*, L8.
(34) Sanganeria, M. K.; Ozturk, M. C.; Violette, K.; Harris, G.; Lee, C. A.; Maher, D. M. *Appl. Phys. Lett.* **1995**, *66*, 1255.
(35) Mogab, C. J. *J. Electrochem. Soc*. **1973**, *120*, 932.
(36) Xia, L.Q.; Engstrom, J. R. *J. Chem. Phys*. **1994**, *101*, 5329.
(37) Itoh, N.; K. Okamoto, K. *J. Appl. Phys*. **1988**, *63*, 1486.
(38) Fissel, A.; Akhtariev, R.; Richter, W. *Thin Solid Films* **2000**, *380*, 42.
(39) Nakamura, S.; Hatayama, T.; Kimoto, T.; Fuyuki, T.; Matsunami, H. *Materials-Science-Forum* **2000**, *338−342*, 201.
(40) Kamins, T. I. *Polycrystalline Silicon for Integrated Circuits Application*; 1988.
(41) Neudorlf, P. S.; Strausz, O. P *J. Phys. Chem*. **1978**, *82*, 241.
(42) Sawrey, B. A.; O'Neal, H. E.; Ring, M. A.; Cofey, D. *Int. J. Chem. Kinet*. **1984**, *16*, 7.
(43) Ikoma, Y.; Endo, T.; Watanabe, F.; Motooka, T. *Appl. Phys. Lett.* **1999**, *75*, 3977.